DOI: https://doi.org/10.36602/jsba.2026.22.35

INVESTIGATION OF CONGO RED'S ADSORPTION MECHANISM ON A BIOSORBENT DERIVED FROM GRAPE LEAVES

Aisha Khalifa Ali Al-Shaltat[1], Abdulfattah Mohamed Alkherraz[2, *], Majed Abdulwahed Alarbish[3], Khaled Muftah Elsherif[4]

[1] Pharmaceutical Technology Department, Faculty of Medical Technology-Misurata, Misurata, Libya
[2] Chemistry Department, Faculty of Science, Misurata University, Misurata, Libya
[3]Office of Biological Sciences Research and Consulting, Research and Consulting Center at Misurata University, Misurata, Libya
[4] Medical Laboratory Sciences Department, Faculty of Health Science, Misurata University, Misurata, Libya
*Corresponding author: Abdoalkherraz@sci.misuratau.edu.ly

Submission data: 18. 7. 2026 Acceptance data: 9/10/2026 Electronic publisher data: 16/10/2026

Abstract: The development of inexpensive, sustainable biosorbents is prompted by the critical environmental issue of adsorption of synthetic dyes from industrial effluents. The purpose of this study is to assess grape leaves that were collected from Misurata, Libya, as a biosorbent for the removal of Congo red dye from aqueous solutions. Batch adsorption experiments were carried out to evaluate the effects of solution pH, contact time, particle size, biosorbent dosage, initial dye concentration, and temperature on adsorption performance. FT IR spectroscopy was used to characterise grape leaf powder. The findings demonstrated that important FT IR bands shift upon dye loading, suggesting their role in Congo red binding. At an initial Congo red concentration of 200 mg/L, an equilibrium adsorption capacity of about 39.92 mg/g was obtained under the selected operating conditions of pH 3.5, a contact time of 30 min, a particle size of 75 µm, and a biosorbent dosage of 0.1 g per 50 mL from 293 K to 333 K, the adsorption capacity increases with temperature, suggesting an endothermic process. With a high correlation coefficient and a calculated equilibrium capacity close to the experimental value, the pseudo-second-order model provided the best fit to the kinetic data among the models evaluated, indicating that it offered the most appropriate empirical description of the adsorption kinetics under the experimental conditions. The Langmuir isotherm provided the best fit among the evaluated models, yielding a theoretical monolayer adsorption capacity (Q_m) of 31.65 mg/g, while the highest experimentally observed equilibrium adsorption capacity was 39.92 mg/g at an initial Congo Red concentration of 200 mg/L. Congo red adsorption onto grape leaf biosorbent is endothermic and becomes easier at higher temperatures, according to thermodynamic analysis, which also revealed decreasing Gibbs free energy and positive enthalpy and entropy changes with temperature. With all factors considered, grape leaves seem to be a viable, inexpensive biosorbent for removing Congo red from tainted water.

Keywords: Congo red, Biosorbent, Isotherms, Kinetics, Thermodynamics

INTRODUCTION

As population expansion, industrialisation, and climate change increase water demand and decline water quality, freshwater supplies worldwide are under growing strain [1], [2]. Large amounts of dye-containing effluents, which are frequently intensely coloured, stable, and resistant to biodegradation, are released by the textile, leather, paper, and plastic sectors. These effluents cause reduced light penetration, oxygen depletion, and ecological imbalance in aquatic systems [3]. Synthetic azo dyes make up the biggest class of these dyes and are especially dangerous since many of them and the byproducts of their degradation can induce cancer and mutagenesis in organisms [4].

A common anionic diazo dye used in paper printing, textile dyeing, and histology staining is Congo Red (CR). Due to its bright colour, great chemical stability, and tendency to produce allergic responses, anaphylactic shock, and carcinogenic or mutagenesis effects in exposed organisms, wastewater containing Congo Red has been identified as a major environmental hazard [5]. It has been demonstrated that the introduction of Congo Red into aquatic environments causes acute toxicity in algae and aquatic animals, with toxicity rising with concentration and duration of exposure. Therefore, effective and affordable ways to eliminate Congo Red from polluted water before disposal are desperately needed [6].

Coagulation-flocculation, electrochemical oxidation, advanced oxidation processes, membrane filtration,

and biological treatment are only a few of the physicochemical and biological methods used for removing dyes [7], [8], [9]. However, a number of these techniques have drawbacks that restrict their widespread use, such as high operating costs, sludge production, sensitivity to process conditions, or insufficient colour removal [10]. Because of its ease of use, high removal efficiency for low and moderate concentrations, and potential for adsorbent regeneration, adsorption has become one of the most efficient and adaptable methods for removing dye from aqueous solutions [11], [12], [13].

The need for inexpensive and sustainable alternatives has been spurred by the high manufacturing and regeneration costs of conventional adsorbents, such as activated carbon, despite their exceptional adsorption ability [14], [15]. Because they are plentiful, affordable, biodegradable, and frequently rich in functional groups (such as hydroxyl, carboxyl, and phenolic groups) that can bind dye molecules, biosorbents made from natural or waste biomass (such as agricultural residues, leaves, peels, and other plant parts) [16] received a lot of attention in this context [17]. Biosorbents made from various plant leaves and agricultural wastes, such as breadfruit, mango, Ficus religiosa, and other lignocellulosic materials, have been used in numerous studies to successfully remove Congo Red. These biosorbents frequently exhibit high adsorption capacities and good agreement with Langmuir isotherm and pseudo-second-order kinetic models [18] .

The adsorption of Congo Red from aqueous solution will be assessed in this work using a biosorbent made from the leaves of the grape vine (Vitis vinifera). In order To better understand the fundamental mechanism and viability of the process, the study will examine how important operational factors affect dye removal and analyse the adsorption process using kinetic, equilibrium isotherm, and thermodynamic models. The current study is to evaluate Vitis vinifera leaf-derived biosorbent as an affordable, effective, and sustainable adsorbent for treating dye-contaminated water, based on earlier research that showed the applicability of leaf-based biosorbents for Congo Red removal.

MATERIALS AND METHODS

Chemicals

All chemicals used in this study were of analytical grade and were used without further purification. Congo red dye with a purity level of at least 98.5% (Merck, Darmstadt, Germany) was used in the experiment. Analytical reagent (AR) grade sodium hydroxide (NaOH) and hydrochloric acid (HCl) were among the reagents supplied by Merck. Deionised (DI) water was obtained from a Millipore-Q system for the experiment.

Collection and preparation of biosorbent

Fresh grape vine (Vitis vinifera) leaves were gathered locally from Misurata, Libya, and properly cleaned using tap water to get rid of dust and adherent pollutants. The leaves were then repeatedly rinsed with distilled water to get rid of soluble contaminants. To guarantee the removal of moisture, the cleaned leaves were air-dried for 72 hours at room temperature and then oven-dried at around 70 °C until a consistent weight was reached. To create various particle size fractions, the dry material was crushed in a lab mill and sieved. These fractions were then kept in airtight containers for use as biosorbent.

Preparation of dye solution

An accurately measured quantity of solid Congo Red was dissolved in distilled water to produce a stock solution of Congo Red dye (1000 mg/L). The stock solution was appropriately diluted with distilled water to produce working solutions with the necessary initial concentrations (5–200 mg/L). A UV-Vis spectrophotometer was utilised to identify the maximum absorption wavelength (λ_{max}) of Congo Red in aqueous solution, which was then utilised for all absorbance measurements [19].

Batch adsorption experiments

Batch adsorption experiments were conducted in 150 mL stoppered conical flasks with a known quantity of biosorbent and a constant amount of dye solution (50 mL). To guarantee even mixing and contact between the dye and biosorbent, the flasks were shaken in a temperature-controlled shaker at a steady speed of 150 rpm. Following the specified contact time, the suspensions were filtered using Whatman filter paper No. 1, and a UV–Vis spectrophotometer (JENWAY 6305 Spectrophotometer) was used to detect the residual dye concentration at Congo Red's λ_{max} [20].

The following formulas were used to determine the percentage removal (%R) of dye and the adsorption capacity at equilibrium, Q_e (mg/g) [21]:

$$\%R = \frac{(C_o - C_e)}{C_o} \times 100 \qquad (1)$$

$$Q_e = \frac{(C_o - C_e) \times V}{M} \qquad (2)$$

In this case, M is the biomass mass (g), V is the solution volume (L), and C_o and C_e stand for the initial and equilibrium dye concentrations (mg/L).

All adsorption experiments were performed in triplicate (n = 3) under identical experimental conditions. The reported values represent the

arithmetic mean of the three independent experimental replicates, and the corresponding standard deviations (SD) were calculated to assess the experimental variability. The results are presented as mean ± SD, and error bars representing the standard deviation are included in the relevant figures.

Effect of experimental parameters

Effect of solution pH:

Before adding the biosorbent, the pH of the Congo Red solutions was adjusted over the range of 3–10 using diluted HCl or NaOH to investigate the effect of initial pH on Congo Red adsorption. During this experiment, the initial dye concentration was fixed at 30 mg/L, the contact time at 30 min, the biosorbent dosage at 0.1 g per 50 mL of dye solution, the particle size at 200–250 µm, and the temperature at 25 °C. The adsorption efficiency was calculated using Equation (2).

Effect of contact time and kinetics:

To investigate the adsorption kinetics of Congo Red onto the grape-leaf biosorbent, experiments were conducted by varying the contact time over the range of 0–50 min. During this experiment, the initial Congo Red concentration was maintained at 30 mg/L, the solution pH was fixed at 3.5, the biosorbent dosage was 0.1 g per 50 mL of dye solution, the particle size was 200–250 µm, and the temperature was maintained at 25 °C. Samples were withdrawn at predetermined time intervals, and the corresponding adsorption capacities (Qt) were calculated. The kinetic data were subsequently fitted to the selected kinetic models.

Effect of particle size:

The effect of biosorbent particle size on Congo Red adsorption was investigated through batch experiments using different particle-size fractions: <0.075 µm, 0.075–0.200 µm, 0.200–0.250 µm, 0.250–0.500 µm, and >0.500 µm. During these experiments, the solution pH was maintained at 3.5, the initial Congo Red concentration was 30 mg/L, the biosorbent dosage was 0.1 g per 50 mL of dye solution, the contact time was 30 min, and the temperature was maintained at 25 °C. The effect of particle size was evaluated under these fixed conditions. In general, smaller particles can enhance adsorption because of their greater specific surface area and shorter diffusion pathways.

Effect of biosorbent dosage:

The effect of biosorbent dosage on Congo Red adsorption was investigated by varying the mass of Vitis vinifera leaf biosorbent from 0.1 to 1.0 g per 50 mL of dye solution. During these experiments, the initial Congo Red concentration was maintained at 30 mg/L, the solution pH was fixed at 3.5, the contact time was 30 min, the particle size was 75 µm, and the temperature was maintained at 25 °C. The effect of biosorbent dosage on the equilibrium adsorption capacity (Qe) was then evaluated under these fixed conditions.

Effect of initial dye concentration and isotherms:

To investigate the equilibrium adsorption behavior and construct the adsorption isotherms, the initial concentration of Congo Red was varied over the range of 5–200 mg/L. All other experimental conditions were maintained constant, including a solution pH of 3.5, a biosorbent dosage of 0.1 g per 50 mL of dye solution, a particle size of 75 µm, a contact time of 30 min, and a temperature of 25 °C. The resulting equilibrium adsorption capacities (Q_e) were used to evaluate the adsorption isotherms.

Effect of temperature and thermodynamic study:

Equilibrium adsorption experiments were conducted at different temperatures (20, 25, 30, 40, 50, and 60 °C) to investigate the temperature dependence and thermodynamic characteristics of Congo Red adsorption. During these experiments, the initial Congo Red concentration was maintained at 30 mg/L, the solution pH was fixed at 3.5, the biosorbent dosage was 0.1 g per 50 mL of dye solution, the particle size was 75 µm, and the contact time was 30 min. The equilibrium constants obtained at the different temperatures were used to calculate the corresponding thermodynamic parameters [22].

Table (1) summarizes the conditions used in each adsorption experiment. The table identifies the parameter varied in each experimental series and specifies the values of the remaining parameters that were kept constant. The selected operating conditions were applied sequentially, such that the conditions identified from the individual parameter studies were subsequently used in the following experiments.

Table 1: Summary of experimental conditions and fixed parameters used in the adsorption experiments.

Experiment	Investigated	pH	Concentration mg/L	Dosage g	Particle size µm	Time min	Temperature °C
pH	3–10	V*	30	0.1	200–250	30	25
Time	0–50 min	3.5	30	0.1	200–250	V*	25
Particle size	<0.075–>0.500 µm	3.5	30	0.1	V*	30	25
Dosage	0.1–1.0 g	3.5	30	V*	75	30	25
Concentration	5–200 mg/L	3.5	V*	0.1 g	75	30	25
Temperature	20–60 °C	3.5	30	0.1 g	75	30	V*

**** Variable***

UV–Vis Spectrophotometric Determination of Congo Red

The concentration of Congo Red in the aqueous solutions was determined using UV–Vis spectrophotometry at its maximum absorption wavelength (λ_{max}) of 490 nm. A calibration curve was established using Congo Red standard solutions over the concentration range of 1–50 mg/L. A linear relationship was obtained between absorbance and Congo Red concentration, expressed by the equation ($y = 0.0203x+0.02$), with a coefficient of determination (R^2) of 0.9992. The calibration equation was subsequently used to determine the Congo Red concentrations in the samples collected from the adsorption experiments.

Adsorption kinetic models

The kinetic data were analyzed using pseudo-first-order and pseudo-second-order models [23].

Pseudo-first-order model (Lagergren):

$$\log (Q_e - Q_t) = \log (Q_e) - \frac{k_1}{2.303} \times t \qquad (3)$$

where Q_t (mg/g) is the adsorption capacity at time t and k_1 (1/min) is the pseudo-first-order model's rate constant.

Pseudo-second-order model:

$$\frac{t}{Q_t} = \frac{1}{k_2 Q_e^2} + \frac{t}{Q_e} \qquad (4)$$

where k_2 (g/mg.min) is the pseudo-second-order rate constant for adsorption and Q_e (mg/g) is the quantity of solute adsorbed at equilibrium.

Adsorption isotherm models

Equilibrium data were fitted to Langmuir, Freundlich, and Temkin isotherm models [24].

Langmuir isotherm:

$$\frac{1}{Q_e} = \frac{1}{Q_m} + \frac{1}{b\, Q_m\, C_e} \qquad (5)$$

where b is the Langmuir isotherm constant (L/mg) and Q_m is the maximal monolayer adsorption capacity (mg/g).

The parameter for dimensionless equilibrium R_L is closely related to the Langmuir model,

$$R_L = \frac{1}{1+b\, C_o} \qquad (6)$$

where C_o stands for the initial dye concentrations. Adsorption type is determined by the R_L value: $R_L = 0$ indicates irreversible adsorption, $0 < R_L < 1$ indicates favourable adsorption, and $R_L > 1$ indicates unfavourable adsorption [25].

Freundlich isotherm:

$$\log Q_e = \log K_F + \frac{1}{n} \log C_e \qquad (7)$$

The heterogeneity component in this model is denoted by 1/n, whereas the Freundlich constant is represented by K_f ($(mg/g)(L/mg)^{1/n}$) [26].

Temkin isotherm:

$$Q_e = B_T \ln K_T + B_T \ln C_e \qquad (8)$$

Here, B_T is the Temkin isotherm constant related to the heat of adsorption, and K_T is the Temkin isotherm equilibrium binding constant (L/g) [27].

Thermodynamic parameters

An essential component of the study of adsorption studies is thermodynamics. The following equations can be used to express the thermodynamic characteristics that determine the process's spontaneity and thermodynamic feasibility: entropy change (ΔS^o), enthalpy change (ΔH^o), and Gibbs free energy (ΔG^o) [24]:

$$\Delta G = \Delta H - T\, \Delta S \qquad (9)$$

$$\Delta G = - RT \ln K_d \qquad (10)$$

For the thermodynamic analysis, the apparent equilibrium constant (K_d) was calculated from the equilibrium concentrations obtained at each temperature. In the present study, the concentration-based equilibrium constant was used to evaluate the

temperature dependence of the adsorption process (equation 11):

$$K_d = \frac{Q_e}{C_e} \qquad (11)$$

The thermodynamic parameters were subsequently determined from the relationship between the equilibrium constant and temperature using the van't Hoff equation (equation 12) [25]:

$$\mathrm{Ln}K_d = \frac{\Delta S}{R} - \frac{\Delta H}{RT} \qquad (12)$$

Equation (12) establishes the relationship between entropy, enthalpy, and K_d.

FT-IR characterization of the biosorbent

The surface functional groups of the grape leaf biosorbent were characterized using Fourier Transform Infrared (FT-IR) spectroscopy (Perkin Elmer Frontier FTIR). The FT-IR spectra of the raw and Congo Red–loaded biosorbent samples were recorded in the wavenumber range 4000–400 cm^{-1} at a resolution of about 4 cm^{-1}.

RESULTS AND DISCUSSION

FT-IR Spectral Characterization Before and After Dye Adsorption

The FT-IR spectrum of the raw grape leaf biosorbent (Figure (1)) shows a broad and intense band around 3338 cm^{-1}, which is attributed to O–H stretching vibrations of hydroxyl groups in cellulose, hemicellulose, lignin, and adsorbed water present in lignocellulosic biomass. The bands observed at approximately 2919 and 2850 cm^{-1}correspond to C–H stretching of aliphatic $–CH_2$ and $–CH_3$ groups in the organic matrix. A distinct band at about 1729 cm^{-1} is assigned to C=O stretching of ester, aldehyde, and carboxylic acid groups, which are typically associated with hemicellulose and surface waxes. The peak near 1607 cm^{-1} is related to aromatic C=C and/or conjugated C=O vibrations from lignin structures, while bands in the region 1421–1317 cm^{-1} are due to C–H bending and O–H bending in the polysaccharide framework. Strong bands around 1057–1024 cm^{-1} are characteristic of C–O–C and C–O stretching in alcohols, ethers, and glycosidic linkages of cellulose and hemicellulose, and the band near 894 cm^{-1} can be attributed to C–H deformation of β-glycosidic bonds or aromatic C–H out-of-plane bending [28], [29].

After adsorption of Congo Red, the FT-IR spectrum of the dye-loaded biosorbent (Figure 2) displays noticeable shifts and changes in intensity of several bands, indicating interactions between dye molecules and surface functional groups. The broad O–H/N–H stretching band shifts from 3338 to about 3296 cm^{-1}, suggesting the involvement of hydroxyl (and possibly amino) groups in hydrogen bonding with dye molecules. The carbonyl band shifts slightly from 1729 to 1733 cm^{-1}, and the aromatic C=C/C=O band moves from 1607 to about 1603 cm^{-1}, which can be associated with complexation or electrostatic interactions between the dye and carboxyl, carbonyl, and aromatic groups of the biosorbent matrix. Bands in the region 1420–1316 cm^{-1} also show minor shifts and intensity variations, further supporting the participation of C–H and O–H groups in the adsorption process. In addition, changes in the C–O/C–O–C stretching region (1242 and 1009–1010 cm^{-1} compared to 1057–1024 cm^{-1} before adsorption) indicate that polysaccharide-type functional groups contribute to dye binding [30].

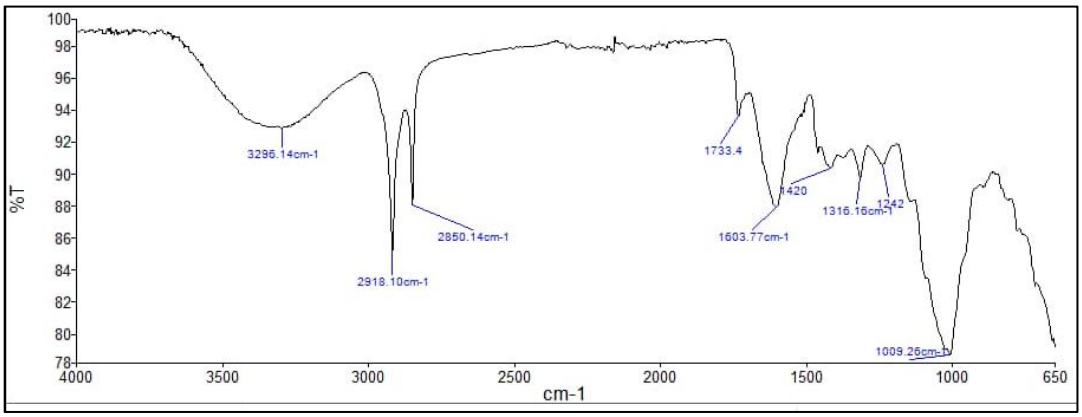


Figure 1: FTIR spectrum for grape leaves before adsorption

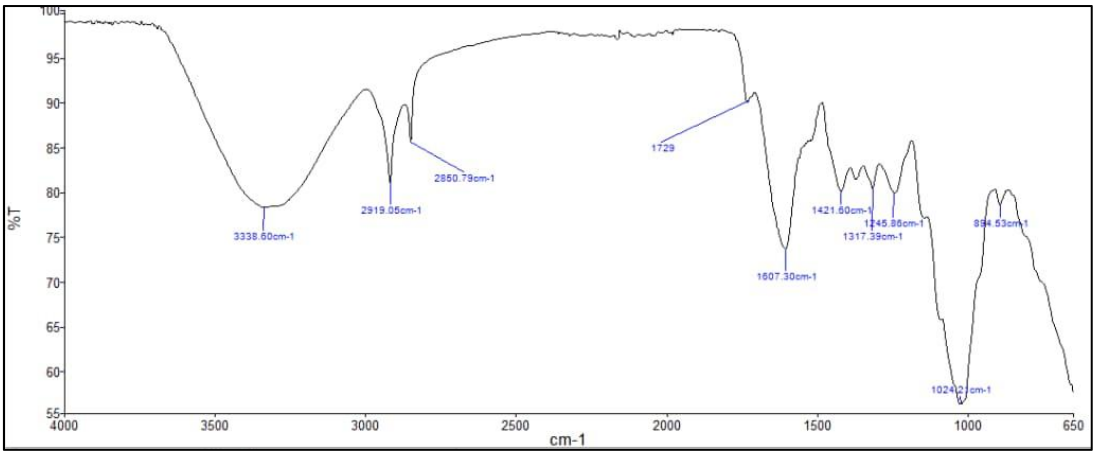


Figure 2. FTIR spectrum for grape leaves after adsorption

Effect of pH on biosorption

Figure (3) shows that the adsorption capacity of grape- leaf biosorbent for Congo red Q_e increases as the solution pH decreases from alkaline to acidic values. In the higher pH range (around pH 9–10), the biosorbent exhibits relatively low uptake (about 4–5 mg/g), whereas Q_e rises progressively as pH is lowered, reaching a maximum of about 9–10 mg/g at pH ≈ 3. This trend indicates that acidic conditions are more favorable for Congo red removal by the prepared biosorbent, which is consistent with many reports on anionic azo dyes [13].

Both the ionic nature of Congo Red and the pH-dependent ionization of functional groups on the grape-leaf biosorbent may contribute to the observed adsorption behavior. Congo Red is an anionic azo dye containing negatively charged sulfonate groups in aqueous solution. Under acidic conditions, protonation of surface functional groups, including hydroxyl, carboxyl, and phenolic groups, can increase the positive character of the biosorbent surface and thereby favor electrostatic attraction toward the anionic dye species. As the pH increases toward neutral and alkaline conditions, progressive deprotonation of surface functional groups may reduce the positive character of the biosorbent and, at sufficiently high pH, promote electrostatic repulsion between the negatively charged surface sites and Congo Red anions. In addition, competition from hydroxide ions for available adsorption sites may contribute to the observed decrease in adsorption capacity at higher pH values. Therefore, the observed pH-dependent adsorption behavior suggests that electrostatic interactions may contribute to Congo Red uptake, in combination with other possible interactions such as hydrogen bonding and π–π interactions, as also reported for Congo Red adsorption onto various biomass-derived adsorbents [31], [32].

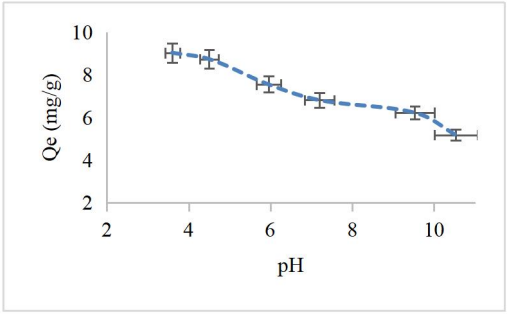


Figure 3: Effect of pH on Congo red adsorption onto grape leaves

Effect of particle size

The impact of particle size on the grape leaf biosorbent's ability to adsorb Congo red is shown in Figure (4). Smaller particles offer better conditions for dye removal, as seen by the consistent drop in equilibrium uptake Qe from around 7.8 mg/g for the smallest fraction (75 µm) to roughly 3.3 mg/g for the coarsest particles (≥ 500 µm). Because a decrease in particle size increases the external surface area and exposes a greater number of accessible adsorption sites, improving mass transfer and surface interaction between dye molecules and functional groups on the adsorbent, this behaviour is frequently seen for lignocellulosic biosorbents. In contrast, larger particles offer a smaller specific surface area and longer intraparticle diffusion paths, which can limit the penetration of dye molecules into the interior of the particles and result in lower adsorption capacities under the same operating conditions [33].

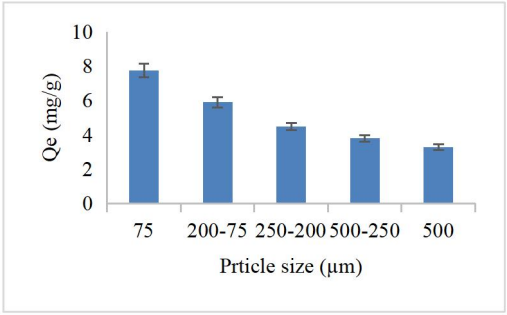


Figure 4: Effect of particle size on Congo red adsorption onto grape leaves

Effect of biosorbent dose

In the range of 0.1–1.0 g, the impact of biosorbent dosage on Congo red adsorption by grape leaf biosorbent was examined (Figure (5)). An inverse relationship between adsorbent dose and Qe was demonstrated by the equilibrium adsorption capacity, which dropped significantly from 4.49 mg/g at 0.1 g to 0.56 mg/g at 1.0 g. Similar trends have been observed for Congo red and other dyes on a variety of inexpensive adsorbents, where an increase in sorbent mass results in a decrease in the amount adsorbed per unit mass [5], [23]. This behaviour is frequently explained by the partial aggregation of particles at larger doses, which lowers the effective surface area and results in active site overlap or crowding, rendering certain adsorption sites inaccessible to dye molecules. Furthermore, even though the overall percentage removal of dye from solution generally increases (from 49% to 65%), the driving force for mass transfer is decreased at high adsorbent doses because a given amount of dye is distributed over a larger number of active sites, leading to lower Q_e values [15]. Thus, lower doses such as 0.1–0.2 g appear more efficient in terms of dye uptake per gram of biosorbent, whereas higher doses may be selected when maximizing total dye removal from the solution is the main objective.

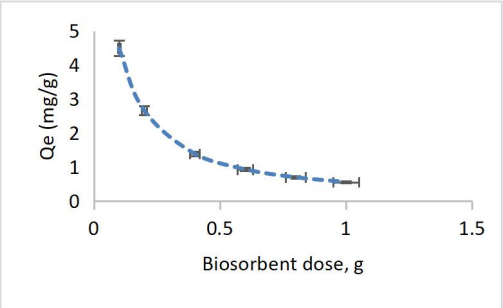


Figure 5: Effect of biosorbent dose on Congo red adsorption onto grape leaves

Effect of contact time

In the range of 0 to 50 minutes, the impact of contact time on Congo red adsorption onto grape leaf biosorbent was assessed (Figure (6)). From 1.37 mg/g at time zero to 3.45 mg/g within 10 minutes and 4.12 mg/g at 20 minutes, the adsorption capacity rose quickly in the early phases, suggesting a quick absorption of dye molecules at the start of the process. The huge number of open and energetically advantageous active sites on the biosorbent surface at the beginning of the experiment, which promotes external mass transfer and Congo red surface binding, is responsible for this quick phase [27]. Q_e values very slightly changed from 4.49 mg/g at 30 minutes to 4.56 mg/g at 50 minutes, as the rate of adsorption steadily reduced and the system neared equilibrium as contact time extended beyond 20–30 minutes. The gradual occupancy of the easily accessible sites, followed by the diffusion of dye molecules into less accessible pores and interior sites within the biosorbent structure, is frequently linked to the sluggish approach to equilibrium [17]. Further increases in contact time did not result in any appreciable improvement in dye absorption, and the practically constant adsorption capacity after 30 minutes indicates that equilibrium was effectively reached at this point.

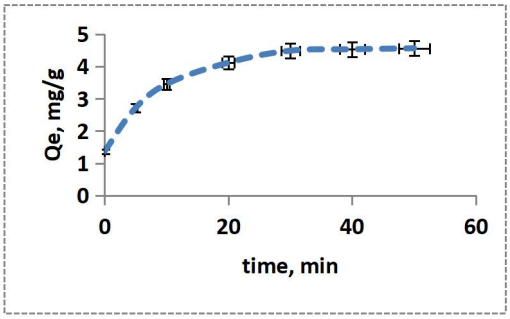


Figure 6: Effect of contact time on Congo red adsorption onto grape leaves

Adsorption kinetics

The adsorption kinetics of Congo red onto the grape-leaf biosorbent were analyzed using the pseudo-first-order and pseudo-second-order models. The linear plot for the pseudo-first-order model (Figure (7a)) showed a moderate correlation, with $R^2 = 0.9586$, and the calculated equilibrium adsorption capacity was Q_e (Cal.) = 1.51 mg/g. Although this model describes the early stages of adsorption to some extent, the relatively lower correlation coefficient and the noticeable difference between the calculated and experimental Q_e values (1.51 and 4.60 mg/g, respectively) indicate that it does not adequately represent the adsorption process. In contrast, the pseudo-second-order model (Figure (7b)) produced an excellent linear fit, with R^2 = 0.9959, and the calculated equilibrium adsorption capacity was Q_e = 4.69 mg/g, which is very close to the experimental value (Q_e (Exp.) = 4.60 mg/g) obtained from the time study. The corresponding rate constant was k_2 = 0.115 $g.mg^{-1}.min^{-1}$, and the initial adsorption rate was h = 2.53 mg $.g^{-1}.min^{-1}$. These results indicate that the pseudo-second-order model provides a better empirical description of the adsorption kinetics of Congo Red onto the grape-leaf biosorbent than the other kinetic models evaluated. The close agreement between the calculated and experimental equilibrium adsorption capacities, together with the higher correlation coefficient, supports the suitability of the pseudo-second-order model for describing the

experimental kinetic data. The good fit of the pseudo-second-order model may also suggest the involvement of chemisorption through specific interactions between Congo Red molecules and active functional groups on the grape-leaf surface. The calculated kinetic parameters for both models are summarized in Table (2).

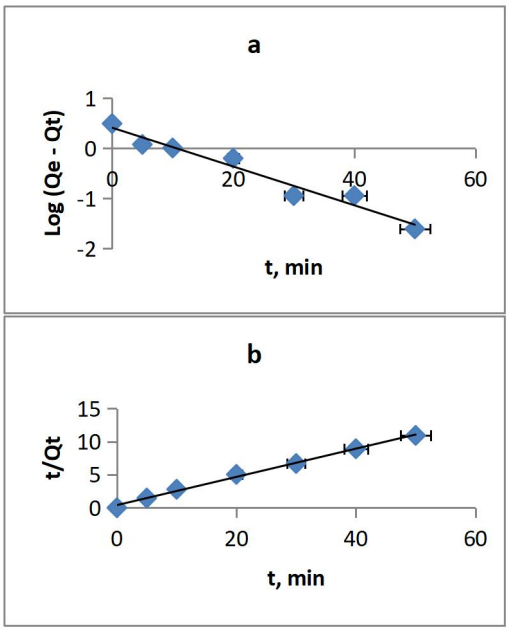


Figure 7: Kinetic model for Congo red biosorption onto grape leaves: a) pseudo-first-order b) pseudo-second-order

Table 2: Kinetic parameters for Congo red biosorption onto grape-leaf biosorbent

Kinetic model	R^2	Rate constant (*k*)	Q_e Cal. (mg/g)	Q_e Exp. mg/g
Pseudo-first-order	0.9586	0.0387 min^{-1}	1.51	4.60
Pseudo-second-order	0.9959	0.115 $g.mg^{-1}.min^{-1}$	4.69	

Effect of dye concentration

The influence of initial Congo red concentration on the adsorption capacity of the grape-leaf biosorbent was investigated over the range 5–200 mg/L. As shown in the plot of C versus Q_e (Figure (8)) the adsorption capacity increased almost linearly with increasing dye concentration, with a very high correlation coefficient (R^2 = 0.994). This behavior indicates that higher concentrations of Congo red provide a stronger driving force for mass transfer between the solution and the biosorbent surface, resulting in greater occupation of available adsorption sites [12]. At low dye concentration, the number of dye molecules in solution is relatively small compared with the number of active sites, so the adsorption capacity remains low [15]. In contrast, as the initial concentration increases, more dye molecules collide with the surface and are retained by the biosorbent, which leads to a progressive increase in Q_e. The nearly linear relationship observed in the present study over the whole concentration range suggests that the grape-leaf biosorbent possesses a high affinity for Congo red and that the active sites were not fully saturated within the studied range [20].

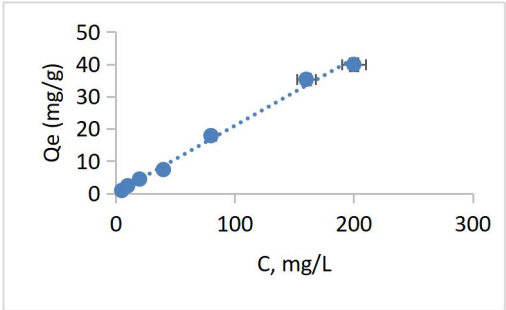


Figure 8: Effect of dye concentration on Congo red adsorption onto grape leaves

Adsorption isotherms

The equilibrium adsorption data of Congo Red onto the grape-leaf biosorbent were analyzed using the linearized forms of the Langmuir, Freundlich, and Temkin isotherm models, as shown in Figures (9a–9c) and summarized in Table (3). Linear regression was applied to the corresponding (C_e) – (Q_e) data according to the linearized equation of each model, and the model parameters were determined from the slopes and intercepts of the respective fitted lines. The coefficient of determination (R^2) was used to assess and compare the goodness of fit of the three isotherm models. The equilibrium isotherm experiments were conducted at 25 °C (298 K). Among the tested models, the Langmuir equation provided the best fit to the experimental data, with the highest correlation coefficient (R^2 = 0.9619), followed by the Freundlich model (R^2 = 0.9523), whereas the Temkin model showed the weakest correlation (R^2 = 0.8393). This indicates that the adsorption behavior of Congo red on the prepared biosorbent is more suitably described by Langmuir-type monolayer adsorption than by the other two models.

The Langmuir model assumes that adsorption occurs on a homogeneous surface with a finite number of identical active sites and that each site binds one dye molecule without interaction between adsorbed species. The calculated maximum monolayer adsorption capacity Q_m was 31.65 mg/g, and the Langmuir constant b was 0.03634 L/mg, indicating a moderate affinity between Congo red and the biosorbent surface. In addition, the separation factor R_L ranged from 0.846 at 5 mg/L to 0.121 at 200

mg/L, confirming that the adsorption process was favorable throughout the studied concentration range, since $0 < R_L < 1$. The good agreement with the Langmuir model suggests that dye uptake was dominated by occupation of a limited number of available surface sites, which is consistent with many biosorption systems reported for Congo red and other dyes. Also, the experimental equilibrium adsorption capacity at the highest initial Congo Red concentration investigated (200 mg/L) reached 39.92 mg/g, whereas the Langmuir model predicted a monolayer adsorption capacity (Q_m) of 31.65 mg/g. Thus, the Langmuir-predicted capacity was approximately 20.7% lower than the highest experimentally observed (Q_e). This difference indicates that the Langmuir model does not reproduce the highest experimental capacity exactly, although it provided the best fit among the isotherm models evaluated based on the applied fitting criterion. The difference may reflect deviations of the experimental adsorption behavior from the ideal assumptions of the Langmuir model, including homogeneous adsorption sites and uniform monolayer coverage.

The Freundlich model also fit the data reasonably well, with $R^2 = 0.9523$, suggesting that surface heterogeneity may contribute to the adsorption process. The Freundlich constant $K_F = 1.076$ and the heterogeneity factor n=1.148 indicate favorable adsorption, since $n > 1$ generally reflects a beneficial interaction between adsorbate and adsorbent. This result implies that although monolayer adsorption appears to be dominant, the biosorbent surface may still contain energetically different sites that participate in dye binding. Such dual behavior is common for lignocellulosic biosorbents, whose surfaces contain a variety of oxygen-containing functional groups from cellulose, hemicellulose, and lignin.

By contrast, the Temkin model showed the poorest fit among the three isotherms, with $R^2 = 0.8393$, indicating that the heat of adsorption is not distributed in a way that strongly supports this model for the present system. The Temkin constant $K_T = 0.661$ and B = 24.495 J/mol suggest only moderate adsorbate–adsorbent interactions, but the lower statistical fit means that Temkin is less suitable for describing the equilibrium behavior of Congo red on grape-leaf biosorbent. Overall, the isotherm analysis shows that Langmuir is the most appropriate model for this system, with Freundlich also providing a reasonable description, while Temkin plays a secondary role in explaining the adsorption mechanism

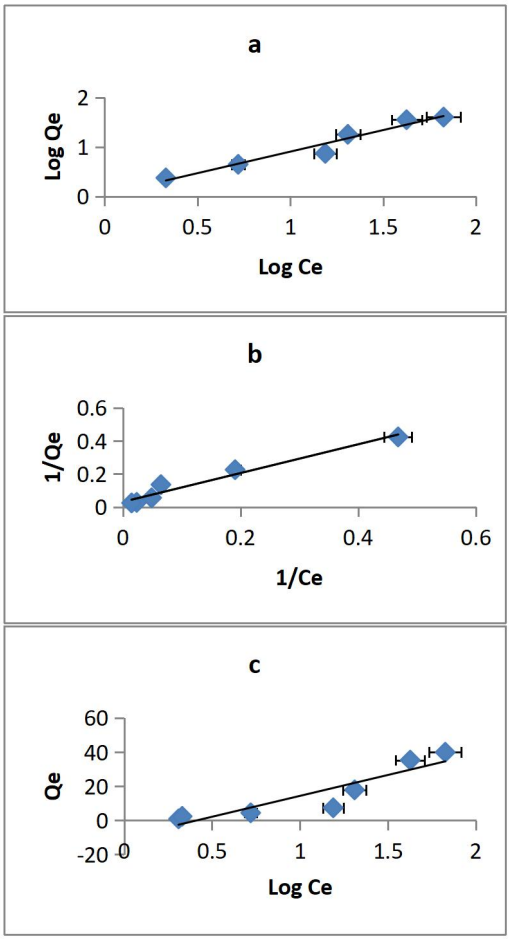


Figure 9: Isotherms models for Congo red biosorption onto grape leaves: a) Freundlich b) Langmuir c) Temkin

Table 3: Calculated Langmuir, Freundlich, and Temkin isotherm parameters for Congo red

Model	Parameter	Value
Freundlich	K_F	1.076 $(mg/g)(L/mg)^{1/n}$
	n	1.148
	1/n	0.871
	R^2	0.9523
Langmuir	Q_m	31.65 mg/g
	b	0.03634 L/mg
	R_L (at 5 mg/L)	0.846
	R_L (at 200 mg/L)	0.121
	R^2	0.9619
Temkin	B	24.495 J/mol
	K_T	0.661 L/mg
	b_T	101.1 J/mol
	R^2	0.8393

adsorption onto grape-leaf biosorbent

Biosorption thermodynamic

The effect of temperature on the adsorption of Congo red onto the grape-leaf biosorbent was investigated in the range 293–333 K (Figure (10)).

The equilibrium adsorption capacity (Q_e) increased progressively from 3.38 mg/g at 293 K to 6.94 mg/g at 333 K, indicating that higher temperatures favor the uptake of Congo red under the studied conditions. This positive temperature dependence suggests that the adsorption process is endothermic in nature, as an increase in temperature enhances the mobility of dye molecules and facilitates their diffusion from the bulk solution to the external and internal active sites of the biosorbent. In addition, the improved Q_e values at elevated temperatures may be attributed to possible structural changes in the biosorbent surface, such as the opening of pores or activation of additional binding sites, which can increase the interaction between Congo red molecules and the functional groups present on the grape- leaf matrix [15], [20].

The thermodynamic parameters governing the adsorption of Congo red onto the grape- leaf biosorbent were evaluated from the temperature-dependent equilibrium data. The van't Hoff plot of $\ln K_d$ versus 1/T (Figure (11)) produced a straight line with a correlation coefficient of 0.9551, indicating that the temperature dependence of the equilibrium constant can be reasonably described by the van't Hoff equation. From the slope and intercept of the linear fit, the standard enthalpy and entropy changes were calculated as $\Delta H° = +31.1$ kJ mol^{-1} and $\Delta S° = +92.9$ J mol^{-1} K^{-1}, respectively. The positive value of $\Delta H°$ confirms that the adsorption of Congo red onto the grape- leaf biosorbent is endothermic, which agrees with the observed increase in adsorption capacity at higher temperatures. The positive $\Delta S°$ suggests an increase in randomness at the solid–solution interface during adsorption, possibly due to the release of water molecules or counter-ions from the biosorbent surface and dye hydration shells as dye molecules occupy the active sites. The standard Gibbs free energy change, calculated from equation 9, decreased from approximately +3.87 kJ mol^{-1} at 293 K to +0.15 kJ mol^{-1} at 333 K. The positive (ΔG^o) values indicate that the adsorption process was thermodynamically non-spontaneous over the investigated temperature range. However, the progressive decrease in (ΔG^o) with increasing temperature indicates that the adsorption became increasingly thermodynamically favorable at higher temperatures, consistent with the endothermic nature of the process. These thermodynamic findings are consistent with the observed enhancement of Congo Red uptake at elevated temperatures and support the favorable effect of increasing temperature on the adsorption process [24,27]. The calculated thermodynamic parameters are summarized in Table 4.

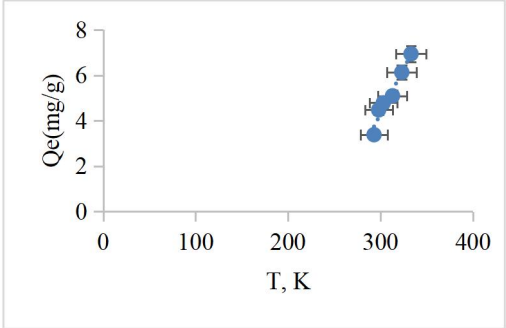


Figure 10: Effect of temperature on Congo red adsorption onto grape leaves

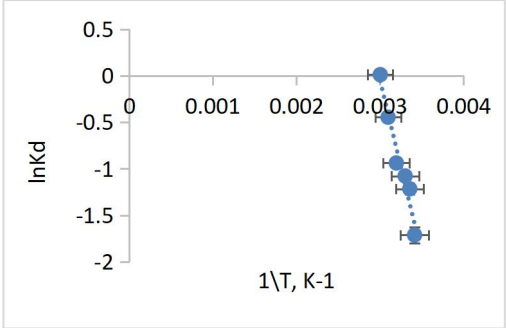


Figure 11: The van't Hoff plot for the adsorption of Congo red onto grape leaves

Table 4: Thermodynamic parameters for the adsorption of Congo red onto grape-leaf biosorbent

T (K)	ΔG^o (kJ/mol)	ΔH^0 (kJ/mol)	ΔS^0 (J/mol. k)	R^2
293	3.87	+31.1	+92.9	0.9551
298	3.40			
303	2.94			
313	2.01			
323	1.09			
333	0.15			

Comparison of Adsorption Performance with Reported Biosorbents

To better assess the performance of the developed biosorbents, the maximum adsorption capacities (Q_{max}) obtained in this study were compared with those reported for other low-cost agricultural and natural adsorbents used for CR removal (Table 5).

Table 5: Comparison of adsorption capacities of selected natural biosorbents for CR dye.

Biosorbent Material	Q_{max}	pH	Time	Dosage	Reference

	(mg/g)		(min)	(g)	
Dry green pea husk Green pea husk charcoal	45.25 2.69	2 2	30 40	0.1 0.1	[10]
Dried fava bean shells Fava bean shell charcoal	14.0 26.0	4 4	30 20	0.1 0.1	[15]
Azadirachta indica leaves	9.98	5	100	0.8	[20]
Peanut shells powder Peanut shells biochar	50.76 64.94	8 5	100 10	0.1 0.1	[34]
Activated carbon prepared from Aloe vera leaves shell	91.0	2	20	0.5	[35]
Vangueria infausta Fruit Pericarp	7.91	2	180	0.7	[36]
Eggshell membrane	112.3	7	60	0.5	[37]
Grape leaves powder	39.9	3.5	30	0.1	Present work

CONCLUSION

The present study demonstrated that grape-leaf biomass is a suitable and effective biosorbent for the removal of the anionic dye Congo red from aqueous solution. Under the selected operating conditions of pH 3.5, a contact time of 30 min, a particle size of 75 μm, and a biosorbent dosage of 0.1 g per 50 mL, an equilibrium adsorption capacity of about 39.92 mg/g was obtained at an initial Congo red concentration of 200 mg/L. These findings confirm that locally available grape leaves, can be valorized as a low-cost adsorbent for dye-contaminated wastewater.

Analysis of the kinetic data showed that the pseudo-second-order model provided the best description of the adsorption process, with a high determination coefficient and a calculated equilibrium capacity in good agreement with experimental values. The pseudo-second-order model provided the best fit to the experimental kinetic data among the models evaluated. Its good agreement with the experimental equilibrium capacity suggests that the model provides an appropriate empirical description of the adsorption kinetics and may indicate the involvement of chemisorption through interactions between Congo Red and active functional groups on the grape-leaf surface. Equilibrium data were best fitted by the Langmuir isotherm, which yielded a monolayer adsorption capacity of 31.65 mg/g and favorable separation factor values over the studied concentration range, indicating monolayer coverage on a finite number of homogeneous sites. The Freundlich and Temkin models also described the data reasonably but with lower correlation, reflecting some surface heterogeneity but a primarily Langmuir-type behavior.

Thermodynamic evaluation revealed positive enthalpy and entropy changes together with a decrease in Gibbs free energy as temperature increased from 293 to 333 K. These parameters confirm that Congo red adsorption onto grape-leaf biosorbent is endothermic and becomes increasingly favorable at higher temperatures, in agreement with the observed rise in adsorption capacity with temperature.

Although the present study demonstrated the promising adsorption performance of grape leaf powder toward Congo red in aqueous solutions, some limitations should be acknowledged. In particular, the biosorbent was evaluated using laboratory-prepared dye solutions rather than actual industrial wastewater. Consequently, the influence of coexisting pollutants, dissolved salts, organic matter, and other matrix components present in real industrial effluents was not assessed. Further studies should therefore investigate the performance of the grape leaf biosorbent using real industrial wastewater under practical operating conditions, as well as its regeneration, reusability, and long-term adsorption performance, to further establish its applicability for wastewater treatment.

ACKNOWLEDGEMENT

The authors sincerely acknowledge the Department of Chemistry, Faculty of Science, Misurata University, for providing the laboratory facilities, equipment, and technical support essential to the successful completion of this study. The authors further express their appreciation to the faculty members and laboratory technicians for their valuable assistance and cooperation throughout the experimental work.

#REFERENCES

1. T. A. Aragaw and F. M. Bogale, “Biomass-based adsorbents for removal of dyes from wastewater: A review,” Front. Environ. Sci.,

vol. 9, art. 764958, 2021, doi: 10.3389/fenvs.2021.764958.

2. K. M. Elsherif, A. El-Hashani, A. El-Dali, and R. El-Kailany, "Bi-ionic potential studies for silver thiosulphate parchment-supported membrane," Int. J. Adv. Sci. Technol. Res., vol. 1, no. 4, pp. 638–646, 2014.
3. T. Islam, M. Repon, T. Islam, et al., "Impact of textile dyes on health and ecosystem: A review of structure, causes, and potential solutions," Environ. Sci. Pollut. Res., vol. 30, pp. 9207–9242, 2023, doi: 10.1007/s11356-022-24398-3.
4. A. Taha and S. Gouda, "Eco-friendly dye removal: Impact of dyes on aquatic and human health and sustainable fungal treatment approaches," Egypt. J. Aquat. Biol. Fish., vol. 29, no. 1, pp. 2733–2763, 2025.
5. K. Manzoor et al., "A comprehensive review on application of plant-based bioadsorbents for Congo Red removal," Biomass Convers. Biorefin., vol. 14, no. 4, pp. 4511–4537, 2024.
6. E. Kağızman, Ş. F. Ergen, and B. E. Taştan, "Evaluation of bioaccumulation and toxicity of Congo Red on Pseudochloris wilhelmii and Daphnia magna," Commun. Fac. Sci. Univ. Ankara Ser. C Biol., vol. 34, no. 1, pp. 36–47, 2025, doi: 10.53447/communc.1656451.
7. C. Martínez-Sánchez, I. Robles, and L. A. Godínez, "Review of recent developments in electrochemical advanced oxidation processes: Application to remove dyes, pharmaceuticals, and pesticides," Int. J. Environ. Sci. Technol., vol. 19, no. 12, pp. 12611–12678, 2022.
8. S. Ledakowicz and K. Paździor, "Recent achievements in dyes removal focused on advanced oxidation processes integrated with biological methods," Molecules, vol. 26, no. 4, art. 870, 2021.
9. N. Y. Donkadokula, A. K. Kola, I. Naz, and D. Saroj, "A review on advanced physico-chemical and biological textile dye wastewater treatment techniques," Rev. Environ. Sci. Biotechnol., vol. 19, no. 3, pp. 543–560, 2020.
10. K. M. Elsherif, A. M. Alkherraz, H. Edwards, and B. Y. A. Mutawia, "Congo Red dye adsorption on dry green pea husk: Effects of process parameters and modeling approaches," Environ. Health Eng. Manag. J., vol. 11, no. 3, pp. 273–284, 2024.
11. S. Moosavi et al., "Application of efficient magnetic particles and activated carbon for dye removal from wastewater," ACS Omega, vol. 5, no. 33, pp. 20684–20697, 2020.
12. E. M. Meshram and S. M. Meshram, "Evaluation of adsorptive capacity of bioadsorbent in removal of Congo Red from aqueous solution," Int. J. Sci. Res., vol. 4, no. 2, pp. 2217–2221, 2015.
13. K. M. Elsherif, A. M. Alkherraz, A. H. Madri, A. Eldali, and M. M. Yaghi, "Kinetic, isotherm, and thermodynamic modeling of methylene blue adsorption by hibiscus plant waste derived biosorbents," J. Chem. Health Risks, vol. 14, no. 4, pp. 727–740, 2024, doi: 10.60829/jchr.2024.1977.
14. K. Y. Foo and B. H. Hameed, "An overview of dye removal via activated carbon adsorption process," Desalin. Water Treat., vol. 19, nos. 1–3, pp. 255–274, 2010.
15. K. M. Elsherif, A. M. Alkherraz, B. Y. A. Mutawia, and A. El-Dali, "Developing biosorbents from agricultural waste: Fava bean shells for efficient dye removal," Eurasian J. Sci. Technol., vol. 6, no. 2, pp. 135–150, 2026, doi: 10.48309/ejst.2026.568396.1296.
16. A. M. Alkherraz, K. M. Elsherif, and A. H. Madri, "Evaluating the efficiency of red tea leaves residues in adsorption of methylene blue dye from liquid wastes: Isotherms, kinetics, and thermodynamics studies," Arab. J. Sci. Res., vol. 5, no. 1, p. 2, 2024, doi: 10.5339/ajsr.2024.2.
17. K. M. Elsherif, A. M. Alkherraz, and A. H. Madiry, "Kinetic isotherm and thermodynamic modelling of methylene blue adsorption using green tea-based biosorbents," Libyan J. Sci., vol. 28, no. 1, 2025.
18. B. M. L. Deepak, P. S. Athira, N. Jayan, D. Barik, and M. S. Dennison, "Preparation of breadfruit leaf biochar for the application of Congo Red dye removal from aqueous solution and optimization of factors by RSM-BBD," Adsorpt. Sci. Technol., 2023, art. 7369027, doi: 10.1155/2023/7369027.
19. K. M. Elsherif, A. El-Dali, A. A. Alkarewi, A. M. Ewlad-Ahmed, and A. Treban, "Adsorption of crystal violet dye onto olive leaves powder: Equilibrium and kinetic studies," Chem. Int., vol. 7, no. 2, pp. 79–89, 2021.
20. T. Javed et al., "Batch adsorption study of Congo Red dye using unmodified Azadirachta indica leaves: Isotherms and kinetics," Water Pract. Technol., vol. 19, no. 2, p. 546, 2024, doi: 10.2166/wpt.2024.020.

21. K. M. Elsherif, A. El-Hashani, and I. Haider, "Equilibrium and kinetic studies of Cu(II) biosorption onto waste tea and coffee powder (WTCP)," Iran. J. Anal. Chem., vol. 5, no. 2, pp. 31–38, 2018.
22. K. M. Elsherif et al., "Kinetics and isotherms studies of safranin adsorption onto two surfaces prepared from orange peels," Moroc. J. Chem., vol. 10, no. 4, pp. 639–651, 2022.
23. E. Güllüce, Y. Gülşahin, G. Karadayı, M. Karadayı, and M. Güllüce, "Bio-removal and detoxification of Congo Red dye in aqueous solutions by using a sustainable biosorbent from Robinia pseudoacacia L.," Int. J. Environ. Res., vol. 20, no. 3, p. 135, 2026.
24. Z. Bensaci, S. Benabdesselam, H. Laksaci, and M. Ramdani, "Efficient removal of Congo Red from wastewater using date-pit activated carbon: Isotherm, kinetic, and thermodynamic studies," Fibers Polym., vol. 27, no. 3, pp. 1285–1297, 2026.
25. A. M. Alkherraz, A. K. Ali, and K. M. Elsherif, "Equilibrium and thermodynamic studies of Pb(II), Zn(II), Cu(II), and Cd(II) adsorption onto mesembryanthemum activated carbon," J. Med. Chem. Sci., vol. 3, no. 1, pp. 1–10, 2020.
26. K. M. Elsherif, A. El-Hashani, and I. Haider, "Biosorption of Fe(III) onto coffee and tea powder: Equilibrium and kinetic study," Asian J. Green Chem., vol. 2, no. 4, pp. 380–394, 2018.
27. B. Souad et al., "Orange seed powder as a novel biosorbent for Congo Red removal: Adsorption mechanism, isotherms, kinetics, and molecular simulations," Molecules, vol. 31, no. 7, art. 1152, 2026, doi: 10.3390/molecules31071152.
28. H. Badamasi et al., "Sustainable removal of Congo Red (CR) dye from aqueous solutions by coagulation–flocculation process using plant-based materials," Sustain. Chem. One World, vol. 100, art. 100204, 2026, doi: 10.1016/j.scowo.2026.100204.
29. T. Bai et al., "Analysis of the performance of composite modified biochar in removing Congo Red dye," Biomass Convers. Biorefin., vol. 16, no. 5, p. 160, 2026, doi: 10.1007/s13399-026-07090-1.
30. D. Manna et al., "Congo Red dye removal using highly porous sulfuric acid activated papaya petiole biochar: Experimental, characterization, optimization and isotherm study," Next Mater., vol. 12, art. 102074, 2026, doi: 10.1016/j.nxmate.2026.102074.
31. K. Csillag, T. Emri, D. E. N. Rangel, and I. Pócsi, "pH-dependent effect of Congo Red on the growth of Aspergillus nidulans and Aspergillus niger," Fungal Biol., vol. 127, nos. 7–8, pp. 1180–1186, 2023, doi: 10.1016/j.funbio.2022.05.006.
32. K. M. Elsherif, A. El-Dali, A. M. Ewlad-Ahmed, A. Treban, and I. Alttayib, "Removal of safranin dye from aqueous solution by adsorption onto olive leaves powder," J. Mater. Environ. Sci., vol. 12, no. 3, pp. 418–430, 2021.
33. X. Ni, Q. Li, K. Yang, H. Deng, and D. Xia, "Efficient degradation of Congo Red by persulfate activated with different particle sizes of zero-valent copper: Performance and mechanism," Environ. Sci. Pollut. Res., vol. 30, no. 27, pp. 70054–70064, 2023, doi: 10.1007/s11356-023-27394-3
34. م.ف.ب. الجروشي، ع.م. الخراز، خ. الشريف. "Study the Adsorption of Congo Rad Dye from its Aqueous Solution on Surfaces Prepared from Peanut Shells," J. Sci. Basic App., vol. 20, pp. 40–52, 2025, doi: 10.36602/jsba.2025.20.40
35. Y.M. Khaniabadi, M.J. Mohammadi, M. Shegerd, S. Sadeghi, S. Saeedi, H. Basiri, "Removal of Congo red dye from aqueous solutions by a low-cost adsorbent: activated carbon prepared from Aloe vera leaves shell," Environ. Health Eng. Manage. J., vol. 4, no. 1, pp. 29–35, 2017.
36. A. Kitemangu, M.R. Vegi, N.M. Malima, L. Yang. "Biosorption of Congo Red Dye from Aqueous Solution Using Adsorbent Prepared from Vangueria infausta Fruit Pericarp," Adsorpt. Sci. Technol., vol. 2023, 2023. doi:10.1155/2023/4319053
37. J. Liu, X. Cheng, P. Qin, M. Pan. "Remove of Congo Red from wastewater by adsorption onto eggshell membrane," Adv. Mater. Res., vol. 599, pp. 391-394, 2012.

دراسة آلية امتزاز صبغة الكونغو الحمراء على ممتز حيوي مشتق من أوراق العنب

عائشة خليفة علي الشلتات[1]، عبدالفتاح محمد الخراز[2]، *، ماجد عبدالواحد الأربش[3]، خالد مفتاح الشريف[4]

[1] قسم علوم الادوية، كلية التقنية الطبية مصراتة، مصراتة، ليبيا
[2] قسم الكيمياء، كلية العلوم، جامعة مصراتة، مصراتة، ليبيا
[3] مكتب الاستشارات والبحوث الحيوية، مركز البحوث والاستشارات جامعة مصراتة، مصراتة، ليبيا
[4] قسم علوم المختبرات الطبية، كلية العلوم الصحية، جامعة مصراتة، مصراتة، ليبيا

الملخص

يأتي تطوير مواد مازة حيوية منخفضة التكلفة ومستدامة استجابةً للمشكلة البيئية الملحّة المتمثلة في إزالة الأصباغ الصناعية من المخلفات السائلة الناتجة عن الأنشطة الصناعية. هدفت هذه الدراسة إلى تقييم أوراق العنب التي جُمعت من مدينة مصراتة، ليبيا، بوصفها مادة مازة حيوية لإزالة صبغة الكونغو الأحمر من المحاليل المائية. أُجريت تجارب امتزاز دفعية لتقييم تأثير كل من الأس الهيدروجيني للمحلول، وزمن التلامس، وحجم الحبيبات، وجرعة المادة المازة الحيوية، والتركيز الابتدائي للصبغة، ودرجة الحرارة في أداء عملية الامتزاز. واستُخدمت مطيافية الأشعة تحت الحمراء بتحويل فورييه (FT-IR) لتوصيف مسحوق أوراق العنب. أظهرت النتائج حدوث تغيرات في مواقع بعض حزم FT-IR المهمة بعد تحميل الصبغة، مما يشير إلى مساهمتها المحتملة في ارتباط صبغة الكونغو الأحمر بسطح المادة المازة. وعند تركيز ابتدائي لصبغة الكونغو الأحمر قدره 200 ملجم/لتر، بلغت سعة الامتزاز عند الاتزان نحو 39.92 ملجم/جرام تحت ظروف التشغيل المختارة، والمتمثلة في أس هيدروجيني قدره 3.5، وزمن تلامس 30 دقيقة، وحجم حبيبات 75 ميكرومتر، وجرعة من المادة المازة مقدارها 0.1 جرام لكل 50 مل. وازدادت سعة الامتزاز بارتفاع درجة الحرارة من 293 إلى 333 كلفن، مما يشير إلى أن عملية الامتزاز ماصة للحرارة. وقدّم نموذج المرتبة الثانية الزائفة أفضل ملاءمة للبيانات الحركية بين النماذج المدروسة، مدعومًا بمعامل ارتباط مرتفع وتقارب السعة الاتزانية المحسوبة من القيمة التجريبية، مما يشير إلى أنه قدّم الوصف التجريبي الأنسب لحركية الامتزاز تحت الظروف المدروسة. كما قدم نموذج لانجمويز أفضل ملاءمة بين نماذج الإيزوثيرم التي جرى تقييمها، حيث أعطى سعة امتزاز أحادية الطبقة نظرية (Q_m) بلغت 31.65 ملجم/جرام، في حين بلغت أعلى سعة امتزاز عند الاتزان تم الحصول عليها تجريبيًا 39.92 ملجم/جرام عند تركيز ابتدائي لصبغة الكونغو الأحمر قدره 200 ملجم/لتر. وأظهرت الدراسة الثرموديناميكية أن امتزاز الكونغو الأحمر على المادة المازة الحيوية المحضرة من أوراق العنب عملية ماصة للحرارة وتصبح أكثر ملاءمة من الناحية الثرموديناميكية مع ارتفاع درجة الحرارة، كما أظهرت انخفاض قيم طاقة جبس الحرة وتغيرات موجبة في كل من الإنثالبي والإنتروبي مع ارتفاع درجة الحرارة. وبالنظر إلى مجمل النتائج، تمثل أوراق العنب مادة مازة حيوية واعدة ومنخفضة التكلفة لإزالة صبغة الكونغو الأحمر من المياه الملوثة.

الكلمات المفتاحية: الكونغو الحمراء، الممتز الحيوي، الأيزوثيرم، الحركية، الديناميكا الحرارية.